AFGL-TR-87-0022

The Importance of Accurate Secondary Electron Yields in Modeling Spacecraft Charging

I. Katz
M. J. Mandell
G. A. Jongeward
M. S. Gussenhoven

S-CUBED
A Division of Maxwell Laboratories
P.O. Box 1620
La Jolla, CA 92038

May 1986

Scientific Report No. 2

AIR FORCE GEOPHYSICS LABORATORY
AIR FORCE SYSTEMS COMMAND
UNITED STATES AIR FORCE
HANSCOM AIR FORCE BASE
MASSACHUSETTS 01731

"This technical report has been reviewed and is approved for publication"

DAVID COOKE
Contract Manager
Spacecraft Interactions Branch
Space Physics Division

CHARLES P. PIKE, Chief
Spacecraft Interactions Branch
Space Physics Division

FOR THE COMMANDER

RITA C. SAGALYN, Director
Space Physics Division

This report has been reviewed by the ESD Public Affairs Office (PA) and is releasable to the National Technical Information Service (NTIS).

Qualified requestors may obtain additional copies from the Defense Technical Information Center. All others should apply to the National Technical Information Service.

If your address has changed, or if you wish to be removed from the mailing list, or if the addressee is no longer employed by your organization, please notify AFGL/DAA, Hanscom AFB, MA 01731. This will assist us in maintaining a current mailing list.

Do not return copies of this report unless contractual obligations or notices on a specific document requires that it be returned.

UNCLASSIFIED
SECURITY CLASSIFICATION OF THIS PAGE

REPORT DOCUMENTATION PAGE

1a. REPORT SECURITY CLASSIFICATION: UNCLASSIFIED	1b. RESTRICTIVE MARKINGS
2a. SECURITY CLASSIFICATION AUTHORITY	3. DISTRIBUTION / AVAILABILITY OF REPORT: Approved for public release; distribution unlimited.
2b. DECLASSIFICATION / DOWNGRADING SCHEDULE	
4. PERFORMING ORGANIZATION REPORT NUMBER(S): SSS-R-87-8474	5. MONITORING ORGANIZATION REPORT NUMBER(S): AFGL-TR-87-0022
6a. NAME OF PERFORMING ORGANIZATION: S-Cubed, A Division of Maxwell Laboratories; 6b. OFFICE SYMBOL (If applicable)	7a. NAME OF MONITORING ORGANIZATION: Air Force Geophysics Laboratory
6c. ADDRESS (City, State, and ZIP Code): P.O. Box 1620, La Jolla, CA 92038	7b. ADDRESS (City, State, and ZIP Code): Hanscom Air Force Base, Massachusetts 01731
8a. NAME OF FUNDING / SPONSORING ORGANIZATION: Air Force Geophysics Laboratory (AFGL/PHK); 8b. OFFICE SYMBOL (If applicable)	9. PROCUREMENT INSTRUMENT IDENTIFICATION NUMBER: Contract F19628-86-C-0056
8c. ADDRESS (City, State, and ZIP Code): Hanscom Air Force Base, MA 01731	10. SOURCE OF FUNDING NUMBERS

PROGRAM ELEMENT NO	PROJECT NO	TASK NO	WORK UNIT ACCESSION NO
62101F	7601	30	AA

11. TITLE (Include Security Classification): The Importance of Accurate Secondary Electron Yields in Modeling Spacecraft Charging

12. PERSONAL AUTHOR(S): I. Katz, M. Mandell, G. Jongeward, M. S. Gussenhoven

13a. TYPE OF REPORT	13b. TIME COVERED	14. DATE OF REPORT (Year, Month, Day)	15. PAGE COUNT
Scientific Report No. 2	FROM ____ TO ____	1986 May	26

16. SUPPLEMENTARY NOTATION

17 COSATI CODES			18. SUBJECT TERMS (Continue on reverse if necessary and identify by block number)
FIELD	GROUP	SUB-GROUP	Spacecraft Charging, SCATHA, Secondary Electrons, POLAR NASCAP, Analytical Modeling

19. ABSTRACT (Continue on reverse if necessary and identify by block number)

Spacecraft charging has commonly been attributed to electrons with several kilovolts of energy impinging upon spacecraft surfaces. Recent experimental evidence from the SCATHA satellite has shown that charging correlates well with electrons of energies greater than 30 keV. In this paper it is shown that the SCATHA observations are consistent with the model of charging in which a satellite is immersed in a Maxwellian plasma, particle collection is orbit limited, and dominant surface effects are the emission of secondary and backscattered electrons. The energy dependence of the secondary yield for multi-kilovolt incident electrons determines the charging threshold. In the past, inadequate representations of the secondary yield have led experimenters to question the validity of the charging model. The accuracy of the secondary electron yield formulation based on electron stopping power, such as the one in the NASCAP and POLAR charging codes, gives good agreement with the SCATHA results. A Maxwellian representation of the magnetospheric plasma is justified by choosing effective temperatures and densities that minimize the error in calculating charging current densities.

20. DISTRIBUTION / AVAILABILITY OF ABSTRACT	21. ABSTRACT SECURITY CLASSIFICATION
☒ UNCLASSIFIED/UNLIMITED ☐ SAME AS RPT. ☐ DTIC USERS	UNCLASSIFIED

22a. NAME OF RESPONSIBLE INDIVIDUAL	22b. TELEPHONE (Include Area Code)	22c. OFFICE SYMBOL
David L. Cooke		AFGL/PHK

DD FORM 1473, 84 MAR — 83 APR edition may be used until exhausted. All other editions are obsolete.

SECURITY CLASSIFICATION OF THIS PAGE
UNCLASSIFIED

Preface

The following paper was started under contract F19628-82-C-0081 and completed under contract F19628-86-C-0056. It addresses the validity of the charging and material models that are incorporated in the POLAR code. In particular, it shows that the observations from the SCATHA satellite and the predictions using the analytical models are consistent.

The authors wish to acknowledge useful discussions with S. T. Lai of Air Force Geophysics Laboratory.

1. Introduction

The first reports of large, negative spacecraft surface potentials in geosynchronous orbit were of eclipse charging (*DeForest* 1972; *Whipple* 1981). The charging was attributed to high fluxes of keV electrons in the absence of photoemission, and explained by the requirement of flux balance between incoming electrons, backscattered electrons, secondary electrons, photoelectrons, and incoming ions. Early efforts to correlate spacecraft potentials with parameters describing the incident electron population used either constants or fits to low energy (0-1000 eV) data to calculate the backscatter and secondary yield coefficients of the spacecraft surface materials. (*Garrett and Rubin*, 1978; *Garrett and DeForest*, 1979; *Garrett et al.*, 1980). These efforts could not consistently predict charging levels.

Subsequently, charging events in excess of one kilovolt negative were measured in sunlight. Sunlight charging is more complex than eclipse charging because of the lack of spatial symmetry. It is clear that additional processes are at work, since first order calculations of the ambient, secondary, and photocurrents produce net postive currents to a magnetospheric satellite. Direct evidence from measured particle spectra, and inferred evidence from modeling efforts, suggest that the formation of potential barriers around the satellite suppress photoemission when the electron environment is sufficiently intense (*Whipple*, 1976a,b; *Olsen et al.*, 1981; *Mandell et al.*, 1978). Generally, a given environment is expected to charge a satellite about an order of magnitude more in eclipse than in sunlight. (*Garrett* (1980) states that "Potentials as high as -2000 V in sunlight and -20,000 V in eclipse have been observed on ATS-6." See also *Purvis* (1983).) This is because, although current balance to a shadowed insulator is the same as that to an eclipsed spacecraft, the charging rate is typically three to four orders of magnitude slower since the insulator must differentially charge relative to underlying grounded metal. It follows that the maximum potential achieved in a

daylight charging event is governed by the duration of the charging environment, and is usually far below the "equilibrium" (steady state) value which might be predicted. *Olsen and Purvis* (1983) discuss the charging dynamics for daylight and eclipse charging events observed on the ATS-5 and ATS-6 spacecraft.

A number of studies have attempted to correlate charging with specific features of observed electron distributions. *Reagan et al.* (1981) found, for the SCATHA satellite, that "surface potentials ... were determined primarily by ... electrons in the energy range < 30 keV and ... that surface charging occurred when the spectrum hardened." *Olsen* (1983) found, in studies of ATS-6 and SCATHA data, that when the electron spectrum hardened his "count rate" commonly exhibited a sharp drop just above its maximum, and that charging occurred when this drop was at an energy exceeding about 15 keV.

Recently, a comprehensive study of high-level sunlight charging events on the SCATHA satellite by *Mullen et al.* (1986) showed that the measured spacecraft-to-plasma potential difference is directly proportional to the intensity of the ambient electron flux greater than 30 keV, and, additionally, that the spacecraft potential is not consistently related to the electron flux below this energy, despite the fact that the low energy flux is commonly an order of magnitude higher than the high energy flux. (Note that the spectra exhibited by *Olsen* (1983) also show significant counts at 30 keV and above, despite a sharp drop in the 10-20 keV range.) A similar relationship between high energy electron flux and spacecraft potential in excess of -100 volts was found for low altitude eclipse charging of DMSP satellites in polar orbit (*Gussenhoven et al.*, 1985). These results were explained in terms of the concept of a critical energy below which the electrons do not contribute to charging because they are self-balanced by their own secondary and backscattered production. The concept of critical energy was quantitatively developed for incident Maxwellian electron distributions by *Lai et*

al. (1983).

The net current density to a satellite, J_{el}^{net}, associated with incident electrons, is found by subtracting backscatter and secondary electrons from the incident electron distribution and integrating over energy. If J_{el}^{net} is negative, the spacecraft will achieve a negative potential such that J_{el}^{net} is balanced by incident ions and ion-produced secondary electrons.

Previous studies by several authors have shown that, for a Maxwellian plasma, charging results only when the electron environment exceeds some threshold temperature (*Stannard et al.*, 1981; *Laframboise and Kamitsume*, 1983). This is because secondary yields typically are greatest for electrons with energies below about 1 keV and are less than unity for electrons with energies above a few keV. Below the threshold, the integral secondary and backscatter yields exceed the incident electron flux, so net charging cannot occur.

Both the study by *Laframboise and Kamitsuma* (1983), and that by *Lai et al.* (1983), indicated charging threshold temperatures of a few keV, and that charging was caused by electrons with energies on the order of 10 keV. These energies are about a factor of three lower than the threshold energy inferred from the SCATHA data (*Mullen et al.*, 1986). As shown below, this discrepancy occurs because the formulation of secondary yields used by these authors was inaccurate and predicted unphysically small secondary yields for electrons in the relevant energy range (5-50 keV).

Lai et al. (1983) and *Laframboise and Kamitsuma* (1983) used an analytical expression for the secondary production given by *Sanders and Inouye* (1979) derived from the work of *Sternglass* (1954). The secondary production predicted is accurate primarily for electrons of low energy (*i.e.*, up to a few keV) but is essentially zero for electron energies greater than 10 keV. Theory (*Alig and Bloom*, 1978) and experiment (*Kanter*, 1961) confirm that secondary yield is

proportional to stopping power for high energy incident electrons. Using secondary formulations which are more correct at high energy, such as those from NASCAP (*Katz et al.*, 1977; *Mandell et al.*, 1984), or that suggested by Burke (*Burke*, 1980), better agreement with the SCATHA observations is obtained.

In the following we formulate a more accurate expression for secondary production from the high energy electron population measured at geosynchronous orbit. We propose a method for selecting Maxwellian parameters from arbitrary distribution functions which best calculates electron charging current densities. The observed strong correlation of charging with the flux of electrons with energy greater than 30 keV and the non-existent (if not negative) correlation with electrons below 30 keV is easily demonstrated when the electron environment is modeled with distributions having constant density and various temperatures.

2. Theory

The theory developed in this section is for a spherical object in an isotropic Maxwellian plasma under eclipsed conditions. However, the conclusions drawn are reasonably general. All quantities are in SI units, with particle energies and plasma temperatures in eV, unless otherwise stated.

The time-dependent charging of an object immersed in a plasma whose total current density to the object is J_{tot} can be described by the equation

$$dV/dt = R\, J_{tot} / \epsilon_0 ,$$

where V is the object to plasma potential difference, R is the effective radius of the object, and ϵ_0 is the permittivity of free space. When in eclipse, the current density J_{tot} consists of

$$J_{tot} = j_{el} + j_{ion} + j_{sec} + j_{back} + j_{prosec} .$$

Here j_{el} and j_{ion} are the incident electron and ion current densities from the

ambient environment, j_{sec} and j_{back} are the electron secondary and backscattered current densities produced by the incident electron current density, and j_{prosec} is the electron secondary current density produced by the incident ion current density. When the incident electron population can be described by a Maxwellian distribution with temperature θ, the secondary (j_{sec}) and backscatter (j_{back}) current densities can be written as integrals over the incident spectrum:

$$j_{sec}/j_{el} = \theta^{-2} \int_0^\infty E \exp(-E/\theta)\, Y(E)\, dE$$

$$j_{back}/j_{el} = \theta^{-2} \int_0^\infty E \exp(-E/\theta)\, B(E)\, dE\ .$$

In these equations Y(E) and B(E) are yield functions for secondary and backscattered production, respectively, taking into account the angular distribution of the incident electrons.

2.1. Secondary Emission Yields

Typical yield of secondary electrons as a function of energy is shown in figure 1. The yield is proportional to the energy deposited by the incident electron in the top 20-100 angstroms of the material. For low energy electrons (with range comparable to or less than this distance) the yield is proportional to the particle energy. At high energy the yield is proportional to the stopping power. This behavior has both a strong theoretical basis and has been verified experimentally (*Kanter*, 1961). The maximum yield occurs in the transition between these two regimes, which is at a few hundred volts for most materials. For spacecraft charging purposes it is important to have a reasonable estimate of secondary yields for 5-50 keV primary electrons. For most materials the electron range is well-represented in this energy regime by a power law:

$$\text{Range} = \text{Constant} \times \text{Energy}^{p}$$

with $1.5<p<2.0$. Since

$$\text{Stopping Power} = [d(\text{Range})/d(\text{Energy})]^{-1}$$

we expect secondary yield to fall off inversely (or slower) with respect to the energy of the primary electron:

$$Y(E) = [E/E_{ext}]^{1-p}$$

where E_{ext} is the energy at which the secondary yield extrapolates to unity. (This is equivalent to the form suggested by *Burke* (1980), who used $p=1.725$. Taking into account that Burke's data is for normal incidence whereas we are interested in isotropically incident electrons, the relation between Burke's constant K and E_{ext} is

$$E_{ext} = (2K)^{1.3793} \text{ [keV]}.$$

The Appendix suggests values of p and E_{ext} for several materials.) Proposed simplified formulas (*Sanders and Inouye*, 1979; *Sternglass*, 1954) having exponential falloffs, while easy to use analytically, will invariably underestimate the yield of secondary electrons for environments capable of charging spacecraft. For most spacecraft materials (which have low atomic number) backscatter yields increase monotonically with energy from zero to a few tenths.

Following *Lai et al.* (1983), E_{upper} is defined as the energy below which electrons do no charging, i.e.,

$$\int_0^{E_{upper}} E \exp(-E/\theta) \, [1-Y(E)-B(E)] \, dE = 0$$

The parameter E_{upper} is a function of θ, being undefined for θ below the charging threshold, infinite at threshold, and reaching a finite limit as $\theta \to \infty$. Assuming the high-energy formula given above for Y(E) and a constant backscatter coefficient, B, this limiting value is

$$E_{upper}(\infty) = E_{ext} \, [(3-p)(1-B)/2]^{1/(1-p)}$$

For Gold subject to isotropically incident electrons, we suggest (based on values developed for NASCAP, *Katz et al.*, 1977; *Mandell et al.*, 1984), the values E_{ext} = 4.6 keV, B = .65, and p = 1.73. We then find E_{upper} = 36 keV. Using the full secondary emission formulation found in NASCAP gives a slightly lower value of 31.2 keV. This contrasts with the 11.1 keV value reported by *Lai et al.* (1983). The threshold Maxwellian temperature for charging is found by NASCAP to be 14.0 keV, compared with 4.9 keV from *Lai et al.* (1983). The low values reported by Lai are due principally to the inadequacy of the secondary formulation used. The backscatter coefficient used here is also somewhat higher than used by *Lai et al.* (1983).

For the purpose of comparison with data from the SCATHA satellite, the electron emission properties are taken to be those of solar cell cover slip model developed for NASCAP (*Mandell et al*, (1984)) since most of the exterior surface of the spacecraft is covered with solar cells. (The results would change little for most typical spacecraft coverings such as teflon beta cloth.) Here the properties E_{ext} = 4.6 keV, B=.32, and p = 1.73, used in the formula above, give a value $E_{upper}(\infty)$ = 14.5 keV. The dashed curve in figure 2 shows the dependence of E_{upper} (calculated using the full NASCAP treatment for secondary and backscatter yields) with the temperature of the ambient environment. The limiting value of E_{upper} by this method is 15.1 keV, and the threshold temperature is 6.8 keV. These are much lower than the corresponding values for Gold, which is a high atomic number material. The average energy of the charging electrons, that is those above E_{upper} weighted by their charging effectiveness is given by

$$E_{charging} = \frac{\int_{E_{upper}}^{\infty} E^2 \exp(-E/\theta)\,[1-Y(E)-B(E)]\,dE}{\int_{E_{upper}}^{\infty} E \exp(-E/\theta)\,[1-Y(E)-B(E)]\,dE}$$

The solid curve in figure 2 shows the dependence of this value on temperature.

Unlike E_{upper}, the average value has an minimum near the threshold temperature. For the SCATHA materials the minimum value is 35 keV at a temperature of 9 keV. The flux of electrons with energies greater than E_{upper} and within θ of the $E_{charging}$ contribute most of the net electron current to the surface and should be a reliable indicator of charging. The choice of $E_{charging}$ is not unique; the median value above E_{upper} would suffice. The basic concept is just that charging is driven by electrons above and within a few θ of E_{upper}.

The quantities E_{upper} and $E_{charging}$ relate to the findings of *Olsen* (1983) and *Mullen et al.* (1986) in the following manner. A given environment will not charge a material if the actual electron spectrum drops significantly below its Maxwellian approximation at an energy much less than the material's E_{upper}; current balance would then be dominated by the secondary electrons produced by the low energy part of the spectrum. Since E_{upper} was calculated above to be 15.1 keV, this explains the finding of *Olsen* (1983) that the requirement for charging is that such a drop occur at 15 keV or higher. Given this, one then expects the spacecraft potential to correlate with the net charging current. By definition, the net charging current consists of that portion of the spectrum with energy above E_{upper}, and is naturally correlated with the differential flux at $E_{charging}$. This explains the finding of *Mullen et al.* (1986) that spacecraft potential is correlated with the flux at 30 keV.

2.2. Single Maxwellian Representation of Environment

The preceding discussion of net current density has been for an assumed Maxwellian distribution of electrons. Data indicates that charging environments are not well fit by a single Maxwellian; frequently two or more Maxwellian descriptions are far superior. The net electron charging current density is in general the integral of the first moment of the velocity distribution function with a

weighting function equal to one minus the secondary plus backscatter yields. That is,

$$J_{el}^{net} = \int_0^{\infty} E\, f(E)\, W(E)\, dE,$$

where $W(E) = [1-Y(E)-B(E)]$. For a Maxwellian distribution the function $f(E)$ is

$$f(E) = N\, e\, \theta^{-2}\, [e\theta/2\pi m_e]^{1/2} \exp(-E/\theta)$$

where N is the number density, m_e and e are the mass and the charge of the electron, respectively. The ideal Maxwellian fit (for charging purposes) would have the property of exactly matching J_{el}^{net}. However, since calculating J_e requires a computer program even for a Maxwellian, a simpler recipe is highly desirable.

In the energy range of interest (a few to fifty keV) the backscatter yield, B(E), depends weakly on energy, while the secondary electron yield Y(E) is reasonably fit by a power law E^{1-p}. Thus we choose a density and temperature which match the incident electron flux and the flux-weighted mean of E^{1-p}. Matching the incident flux assures a reasonably close value for the weakly energy dependent [1-B(E)] portion of the integral for J_e, while the other condition gives a good match for the mean secondary electron yield. For a Double Maxwellian with densities N_A, N_B, and temperatures θ_A, θ_B, respectively, we define

$$F_A = N_A\, \theta_A^{1/2}\,;\; F_B = N_B\, \theta_B^{1/2}\,.$$

Then, it can be shown that the single Maxwellian which fits our criteria has temperature and density given by

$$\theta^{1-p} = (F_A/(F_A+F_B))\theta_A^{1-p} + (F_B/(F_A+F_B))\theta_B^{1-p}$$
$$N = [F_A+F_B]\theta^{-1/2}\,.$$

We have applied this scheme to fifty-three Double Maxwellian environments measured by the SCATHA spacecraft, as quoted by *Schnuelle et al.* (1981). We used the value p=1.73, appropriate to the NASCAP model for solar cell

coverslips, as well as many other common spacecraft materials. The full NASCAP formulations for secondary and backscatter yield were then used to calculate J_{el}^{net} for each Double Maxwellian environment and its single Maxwellian representation. Defining the error as the difference in J_{el}^{net} divided by the incident electron flux, we found the root-mean-square error to be 3.7 percent, with the maximum error 9.2 percent. The larger errors were for environments below the threshold for charging. The five environments capable of charging this material had a root-mean-square error of 0.6 percent.

By this procedure the equivalent Maxwellian temperature for charging is material dependent through the range exponent p. However, since the variation in p is not great, this material dependence is fairly slight. Also, since secondary electrons produced by ions are proportional to the ion velocity, the value p=1/2 should be used to compute the equivalent Maxwellian temperature for an ion spectrum.

2.3. Application to Spacecraft Charging

We will now show that the above considerations predict a positive correlation between spacecraft potential and measured electron flux with energy in excess of 30 keV, and a null (or even negative) correlation with electron flux below 30 keV (or, equivalently, total electron flux).

Consider the charging response of an idealized satellite in a neutral isothermal Maxwellian hydrogen plasma. The satellite is assumed to be a spherical probe that collects ion and electron currents according to orbit limited theory. That is, net current densities resulting from the incident electron and ion distributions are

$$J_{el}^{net} = \int_0^\infty E\, f_e(E\text{-}V)\, W(E)\, dE,$$

$$J_I = \int_{-V}^{\infty} E\, f_I(E+V)\, W_I(E)\, dE$$

where V is the spacecraft potential (assumed negative), $W_I(E)$ is unity plus the secondary electron emission coefficient for incident ions, and

$$f_\alpha(E) = N_\alpha\, e\, \theta^{-2}\, [e\theta/2\pi m_\alpha]^{1/2} \exp(-E/\theta)$$

The equilibrium potential is found by integrating in time the basic charging equation until a steady value is obtained. (The time scale for approach to steady state is milliseconds for typical magnetospheric plasmas.) The equilibrium floating potential is a monotonic function of the plasma temperature.

For a fixed plasma density of 1 cm^{-3} the equilibrium satellite potential was calculated for plasma temperatures ranging from 8 to 20 keV in steps of one kilovolt. Also calculated was the incident electron flux in the two energy ranges of the instrument on SCATHA reported in *Mullen et al.* (1986). The low energy channel was taken to be all electrons between 50 eV and 30 keV the high channel was from 30 keV to 400 keV.

In Figure 3 the circles indicate spacecraft potential as a function of the high energy flux, the plus signs the potential vs the low energy flux. Each pair of circles and crosses at a single potential are results from a single temperature. The obvious positive correlation of the potential with high energy flux and the small, negative correlation with the low energy flux are in good agreement with the SCATHA data from *Mullen et al.* (1986). (The scale of the potential here is an order of magnitude greater, because this analysis was performed for eclipse charging, while the published observations are for sunlight charging.) The incident electron current in all cases of charging is balanced by a combination of incident ions and secondary and backscattered electrons.

3. Discussion

The observation that charging correlates directly with the flux of electrons with energies greater than 30 keV is completely consistent with the description of charging as the balancing of incident electron currents by secondary emission, backscatter and ion currents. Previous analysis by *Lai et al.* (1983) had assumed the material properties were that of gold, a highly emissive material, but still came up with lower than the observed energies. The present work is in much better agreement with experiment for two reasons. First, and certainly most important, the formulation of the secondary yield as a function of energy used here is much more accurate for incident electron energies greater than a few keV. Second, the definition of the mean energy of the charging electrons is more relevant than that of the lowest energy electron to contribute to charging, since the bulk of the charging current is near the mean. The fundamental mechanisms leading to spacecraft charging are the same for both works, namely, the achievement of current balance. However, it points out just how critical is the accurate knowledge of both material properties and the ambient environment for both high and low energies if modeling efforts are to give good spacecraft potential predictions. While this paper used a single Maxwellian representation of the charging environment, the results are applicable to other energy distributions since charging involves integrals over the distribution and is not particularly sensitive to details of the shape of the distribution function. The prediction of the energy channel which will indicate charging will vary little for well behaved monotonic spectra. The good agreement with SCATHA results from having a good representation of the material properties and the high energy electron environment. Use of a single Maxwellian to represent the highly variable magnetospheric environment is convenient, but not essential.

Appendix

Suggested Constants for Several Materials

The table below gives, for several materials, suggested values for the range exponent p, the energy, E_{ext}, at which secondary yield extrapolates to unity, approximate backscatter coefficient, B (evaluated at 10 keV), and resultant limiting value of E_{upper} from the formula

$$E_{upper}(\infty) = E_{ext}\,[(3\text{-}p)(1\text{-}B)/2]^{1/(1-p)}$$

Values from *Burke* (1980) have been doubled to account for isotropic incidence.

Material	p	E_{ext}[keV]	B	E_{upper}[keV]
Aluminum	1.76 (B)	1.8 (B)	.36(B)	6
Carbon (Aquadag)	1.55 (B)	1.2 (B)	.27(B)	4
Gold	1.73 (B)	4.6 (B)	.64(B)	35
Kapton	1.725(A)	1.53(A)	.25(B)	4
Lucite	1.725(A)	3.02(A)	.14(A)	7
Magnesium	1.75 (B)	.7 (B)	.35(B)	2
Mylar	1.725(A)	2.07(A)	.14(A)	5
Nylon	1.725(A)	3.15(A)	.14(A)	7
Polyethylene	1.725(A)	4.02(A)	.14(A)	9
Polystyrene	1.725(A)	2.27(A)	.14(A)	5
Polyvinylalcohol	1.725(A)	3.51(A)	.14(A)	8
Silver	1.74 (B)	4.0 (B)	.55(B)	22
SiO_2	1.86 (B)	4.8 (B)	.33(B)	15
SOLA	1.73 (B)	4.63(B)	.33(B)	15
Teflon	1.725(A)	4.75(A)	.29(B)	14

(A) *Burke* (1980)

(B) NASCAP *(Katz et al.*, 1977; *Mandell et al.*, 1984)

References

Alig, R. C., and S. Bloom, "Secondary-Electron-Escape Probabilities", *Journal of Applied Physics 49*, 3476-3480, 1978.

Burke, E. A., "Secondary Emission from Polymers", *IEEE Transactions on Nuclear Science NS-27*, 1760-1764, 1980.

DeForest, S. E., "Spacecraft Charging at Synchronous Orbit", *Journal of Geophysical Research 77*, 651, 1972.

Garrett, H. B. and S. E. DeForest, "Time-varying Photoelectron Flux Effects on Spacecraft Potential at Geosynchronous Orbit", *Journal of Geophysical Research 84*, 2083, 1979.

Garrett, H. B. and A. G. Rubin, "Spacecraft Charging at Geosynchronous Orbit - Generalized Solution for Eclipse Passage", *Geophysical Research Letters 5*, 865, 1978.

Garrett, H. B., D. C. Schwank, P. R. Higbie, and D. N. Baker, "Comparison between the 30- to 80- keV Electron Channels on ATS-6 and 1976-058A During Conjunction and Application to Spacecraft Charging Predictions", *Journal of Geophysical Research 85*, 1155, 1980.

Garrett, H. B., "Spacecraft Charging: A Review", in *Space Systems and Their Interactions with the Earth's Space Environment*, H. B. Garrett and C. P. Pike, ed., pp. 167-226, AIAA, 1980.

Gussenhoven, M. S., D. A. Hardy, F. Rich, W. J. Burke, and H.-C. Yeh, "High-level Spacecraft Charging in the Low-Altitude Polar Auroral Environment", *Journal of Geophysical Research 90*, 11,009, 1985.

Kanter, H., "Energy Dissipation and Secondary Electron Emission in Solids", *Physical Review 121*, 677, 1961.

Katz, I., D. E. Parks, M. J. Mandell, J. M. Harvey, D. H. Brownell, S. S. Wang, M. Rotenberg, *A Three Dimensional Dynamic Study of Electrostatic Charging in Materials*, NASA CR-135256, S-CUBED Report SSS-R-77-3367, 1977.

Laframboise, J. G., and M. Kamitsuma, "The Threshold Temperature Effect in High-Voltage Spacecraft Charging", *Proceedings of the Air Force Geophysics Laboratory Workshop on Natural Charging of Large Space Structures in Near Earth Polar Orbit: 14-15 September 1982, AFGL-TR-83-0046*, pp. 293-308, 1983. ADA134894.

Lai, S. T., M. S. Gussenhoven and H. A. Cohen, "The Concepts of Critical Temperature and Energy Cutoff of Ambient Electrons in High Voltage Charging of Spacecraft", *Proceedings of the 17th ESLAB Symposium on Spacecraft/Plasma Interactions and their Influence on Field and Particle Measurements, Noordwijk, The Netherlands, 13-16 Sept. 1983, ESA sp-198*, pp. 169-175, 1983.

Mandell, M. J., I. Katz, G. W. Schnuelle, P. G. Steen, and J. C. Roche, "The Decrease in Effective Photocurrents due to Saddle Points in Electrostatic Potentials near Differentially Charged Spacecraft", *IEEE Transactions on Nuclear Science NS-25*, 1313, 1978.

Mandell, M. J., P. R. Stannard, and I. Katz, *NASCAP Programmer's Reference Manual* S-CUBED Report SSS-84-6638, 1984.

Mullen, E.G., M. S. Gussenhoven, D. A. Hardy, T. A. Aggson, B. G. Ledley and E. Whipple, "SCATHA Survey of High Level Spacecraft Charging in Sunlight", *Journal of Geophysical Research 91*, 1474, 1986.

Olsen, R. C. "A Threshold Effect for Spacecraft Charging", *Journal of Geophysical Research 88*, 493, 1983.

Olsen, R. C. and C. K. Purvis, "Observations of Charging Dynamics", *Journal of Geophysical Research 88*, 5657, 1983.

Olsen, R. C., C. E. McIlwain, and E. C. Whipple, Jr., "Observations of Differential Charging Effects on ATS-6", *Journal of Geophysical Research 86*, 6809, 1981.

Purvis, C. K., "The Role of Potential Barrier Formation in Spacecraft Charging", *Proceedings of the 17th ESLAB Symposium on Spacecraft/Plasma Interactions and their Influence on Field and Particle Measurements, Noordwijk, The Netherlands, 13-16 Sept. 1983, ESA sp-198*, pp. 115-124, 1983.

Reagan, J. B., R. W. Nightingale, E. E. Gaines, R. E. Meyerott, and W. L. Imhof. "The Role of Energetic Particles in the Charging/Discharging of Spacecraft Dielectrics", *Spacecraft Charging Technology-1980*, NASA CP-2182, AFGL-TR-81-0270, 493-499, 1981. ADA114426.

Sanders, N. L. and G. T. Inouye, "Secondary Emission Effects on Spacecraft Charging: Energy Distribution Consideration", *Spacecraft Charging Technology-1978 NASA CP2071/AFGL-TR-79-0082*, pp. 747-755, 1979. ADA084626.

Schnuelle, G. W., P. R. Stannard, I. Katz, and M. J. Mandell, "Simulation of Charging Response of SCATHA (P78-2) Satellite", *Spacecraft Charging Technology-1980*, NASA CP-2182, AFGL-TR-81-0270, 580-591, 1981. ADA114426.

Stannard, P. R., G. W. Schnuelle, I. Katz, and M. J. Mandell, "Representation and Material Charging Response of GEO Plasma Environments " Spacecraft Charging 1980, NASA CP-2182, AFGL-TR-81-0270, 560-579, 1981. ADA114426.

Sternglass, E. J., "Theory of Secondary Electron Emission", *Physical Review 95*, 345-358, 1954.

Whipple, E. C., Jr., "Theory of the Spherically Symmetric Photoelectron Sheath: A Thick Sheath Approximation and Comparison with the ATS-6 Observation of a Potential Barrier", *Journal of Geophysical Research 81*, 601, 1976a.

Whipple, E. C., Jr., "Observations of Photoelectrons and Secondary Electrons Reflected from a Potential Barrier in the Vicinity of ATS-6", *Journal of Geophysical Research 81*, 715, 1976b.

Whipple, E. C., "Potentials of Surfaces in Space", *Reports on Progress in Physics 44*, 1197, 1981.

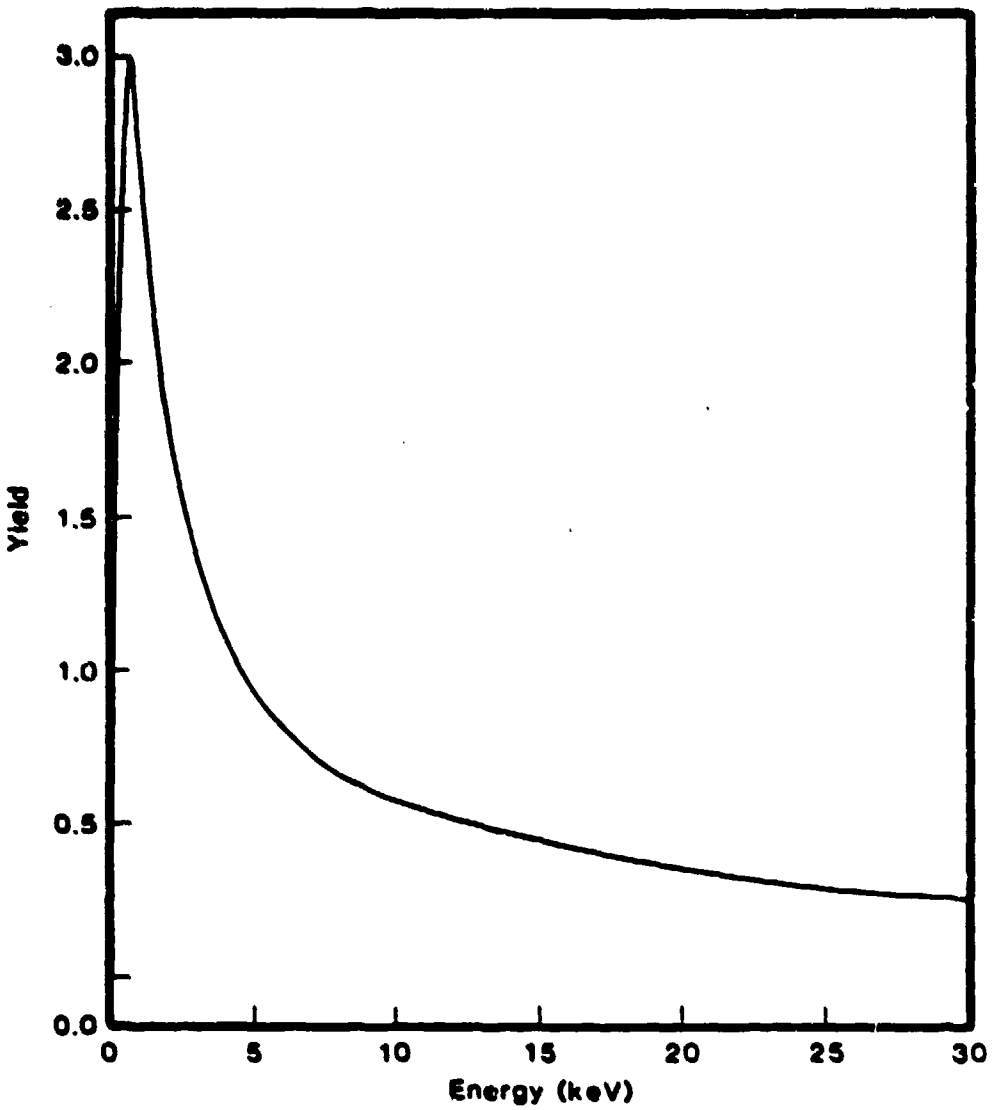

Figure 1. Secondary yield vs. primary electron energy for solar cell coverslip material, assuming isotropic incidence.

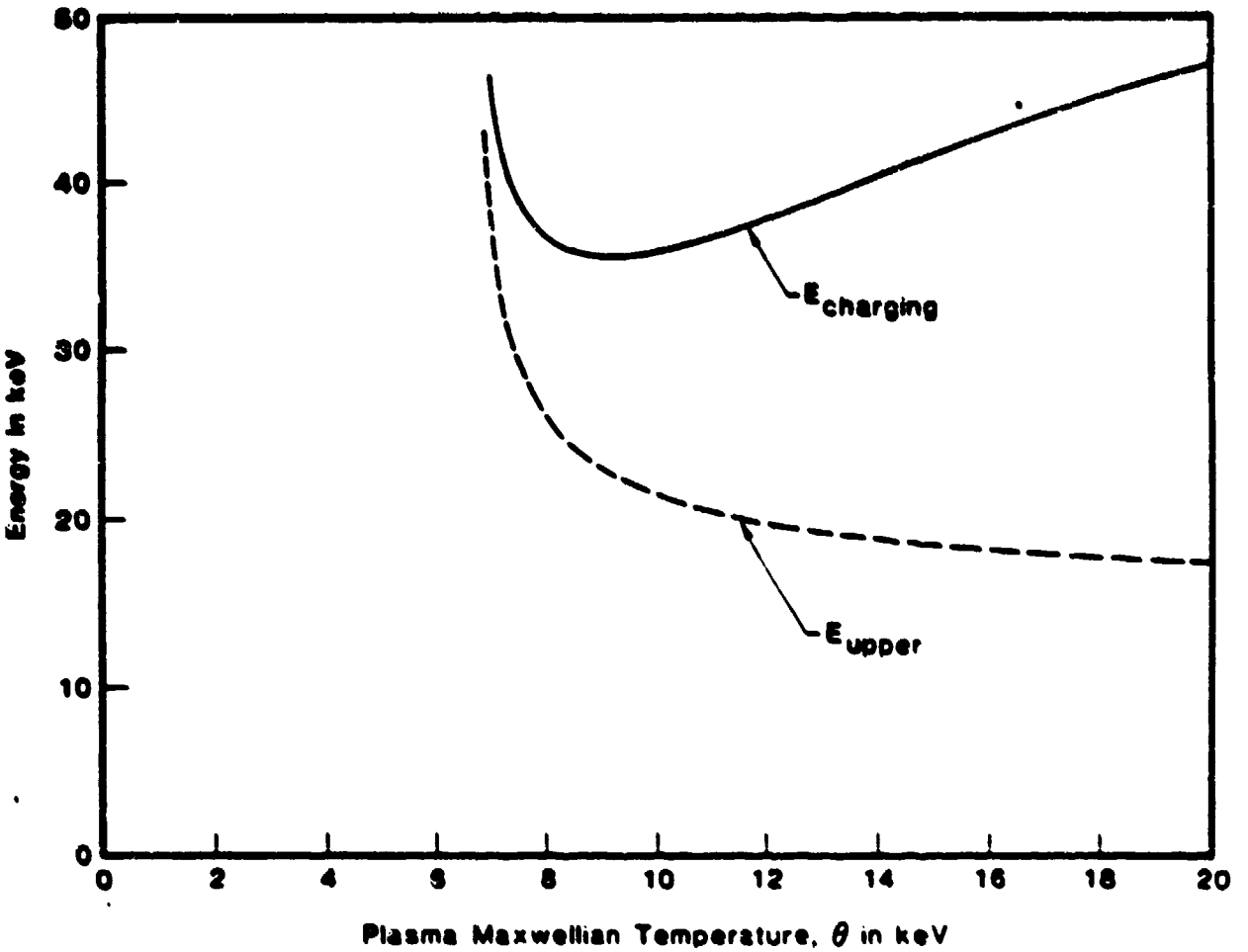

Figure 2. E_{upper} (dashed curve) and $E_{charging}$ (solid curve) as functions of assumed Maxwellian temperature

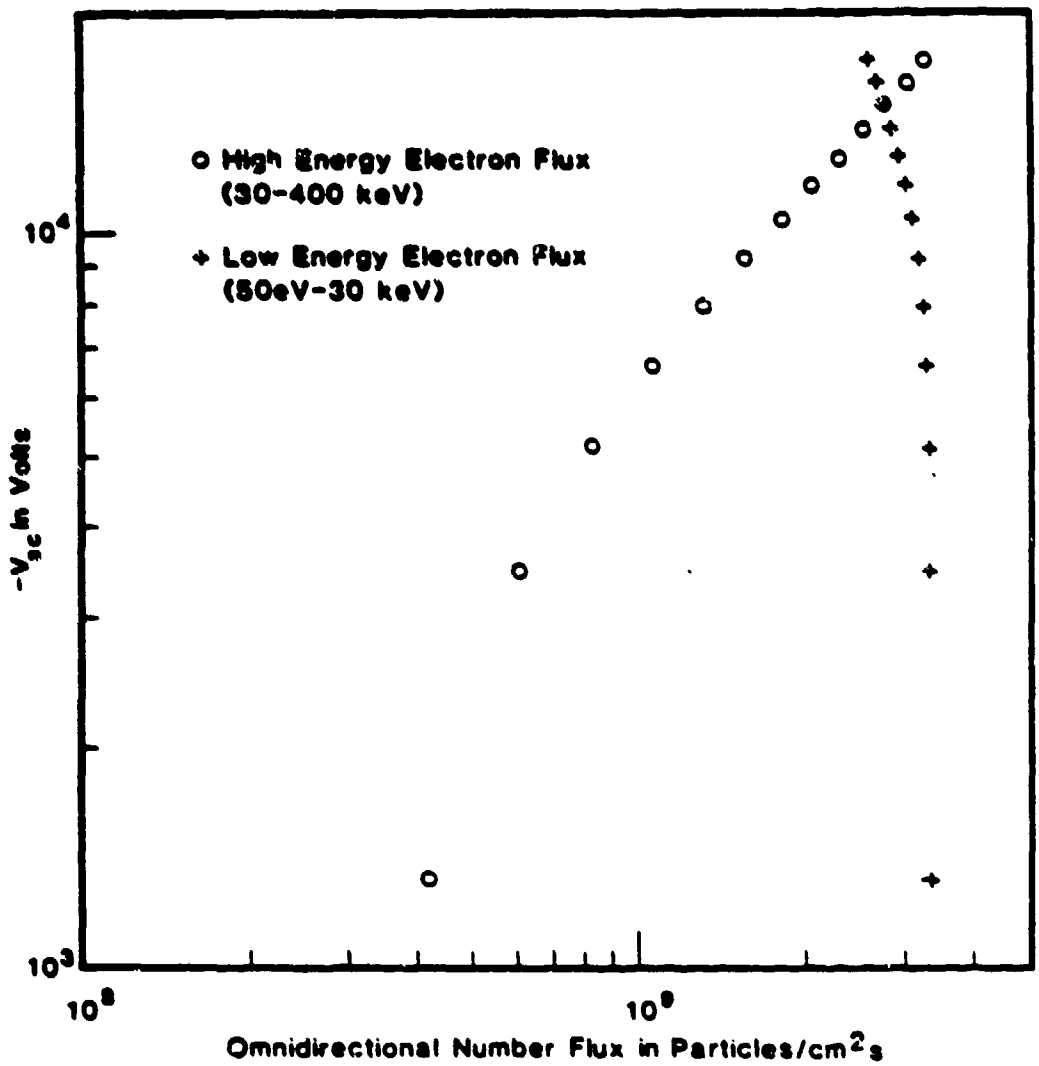

Figure 3. Spacecraft potential as functions of low energy (+) and high energy (o) omnidirectional electron fluxes for a fixed plasma density. The Maxwellian temperature ranged from 8 to 20 keV.